ISSN: 1410-8917
Jurnal Kimia Sains & Aplikasi
e-ISSN: 2597-9914

Jurnal Kimia Sains dan Aplikasi 28 (5) (2025): 260-266
Jurnal Kimia Sains dan Aplikasi
Journal of Scientific and Applied Chemistry
Journal homepage: http://ejournal.undip.ac.id/index.php/ksa

Adsorption of Methyl Red Dye on Fixed-Bed Column Using Bottom Ash Adsorbent from Palm Oil Mill Waste

Novi Sylvia [1,*], Rozanna Dewi [1], Fikri Hasfita [1], Leni Maulinda [1], Wusnah [1], Azhari [1], Zikri Husni Sigian [1], Balqis Eka Putri [1], Fitriani [2]

[1] Department of Chemical Engineering, Malikussaleh University, Lhokseumawe, 24351, Indonesia
[2] Medical Informatics, FKTS, Bumi Persada University, Lhokseumawe, Aceh, Indonesia

* Corresponding author: novi.sylvia@unimal.ac.id

https://doi.org/10.14710/jksa.28.5.260-266

Article Info

Article history:

Received: 19th February 2025
Revised: 19th June 2025
Accepted: 23rd June 2025
Online: 10th July 2025

Keywords:
Adsorption; methyl red; fixed-bed; bottom ash; low-cost

Abstract

Methyl red is an azo compound widely applied in the textile industry as a fabric dye. Methyl red is very difficult to decompose because it is stable to light, temperature, and oxidation. One of the simplest and low-cost methods is adsorption. This study aims to determine the characteristics of bottom ash as an adsorbent and analyze the adsorption process with a fixed-bed column system. The research was conducted by varying the flow rate of 5, 10, and 15 L/min, adsorbent bed height of 4, 8, and 12 cm, and contact time of 60, 120, and 180 minutes. The highest removal efficiency, 93%, was achieved at a contact time of 180 minutes, a flow rate of 5 L/min, and a bed height of 12 cm. The physical properties of the bottom ash adsorbent include a pore volume of 0.0032 cm^3/g, a specific surface area of 89.801 m^2/g, and an average pore size of 58.523 nm. The maximum adsorption capacity was found to be 0.850 mg/g. The adsorption process of methyl red onto bottom ash follows the Langmuir isotherm model.

1. Introduction

The largest manufacturing industry in Indonesia is currently the textile industry, which has seen significant growth due to its promising prospects and national priority status [1]. The textile production process, which involves multiple stages, generates various types of waste, including solid, liquid, and gaseous waste. In particular, liquid waste from the dyeing process contains high ammonia levels, posing a risk of water pollution. One of the commonly used dyes in the textile industry is methyl red (MR) [2, 3].

Most textile dyes are derived from azo compounds and benzene derivatives, which are highly resistant to degradation. Textile mills consume large amounts of water in processes such as bleaching, dyeing, and washing, often discharging untreated wastewater into water bodies. This wastewater primarily contains organic dyes that disperse well in water, making their removal challenging using conventional methods. The presence of these dyes alters water coloration, negatively impacting the visual landscape [4].

Additionally, high dye concentrations reduce light penetration into aquatic environments, lowering photosynthesis rates and decreasing oxygen levels essential for aquatic flora and fauna. Many organic dyes exhibit toxic, mutagenic, and carcinogenic properties. In developing countries, dye-contaminated water is often used for irrigation, further spreading pollution. These dyes contaminate irrigation water and disrupt soil microbial activity, negatively impacting soil health and fertility [5].

Various methods have been employed to treat textile industry effluents and mitigate environmental pollution. Common wastewater treatment techniques include electrocoagulation, chemical oxidation, ozonation, membrane degradation, and filtration. Among these, adsorption is widely recognized as an effective, simple, and cost-efficient technique [1, 3, 6, 7, 8].

The effectiveness of adsorption largely depends on the choice of adsorbent, as it influences the purification process [5, 8, 9, 10, 11]. A key characteristic of an effective adsorbent is its surface area, as a larger surface area enhances adsorption capacity by providing more active sites for adsorbate interaction [7, 8]. Various adsorbents have been studied for MR removal, including activated carbon, zeolite, mesoporous silica, and biomass-based materials.

Biomass waste-derived adsorbents, such as oil palm waste (e.g., palm shells and fibers), are commonly preferred for commercial applications. Many factories use palm shells and fibers as boiler fuel, producing bottom ash as a byproduct. Bottom ash consists primarily of silica (SiO_2) and alumina (Al_2O_3), the main components of zeolite. Since zeolites are known for their MR adsorption capacity, bottom ash, with a similar composition, also has the potential to act as an effective adsorbent for MR removal [11, 12, 13, 14].

Research on bottom ash-based adsorbents has primarily focused on heavy metal adsorption, with limited studies on MR adsorption. Currently, bottom ash remains underutilized and poorly managed, posing a challenge for the palm oil industry due to its increasing accumulation and the large storage areas required [15]. Malviya *et al.* [16] and Savcı and Uysal [17] have explored the use of bottom ash for methyl orange adsorption. Utilizing bottom ash as an adsorbent presents a sustainable approach to mitigating environmental pollution [8, 15, 18].

In the palm oil industry, bottom ash from combustion residues is often left in accumulated piles, leading to potential groundwater contamination [19]. Consequently, various innovations have been developed to repurpose bottom ash, including its use as a cement substitute and an adsorbent. This study investigates the potential of bottom ash as an adsorbent for MR removal using a column system, following an initial characterization of its properties.

2. Experimental

2.1. Materials and Equipment

This adsorption study utilized bottom ash obtained from PT IBAS palm oil mill in North Aceh Regency, along with distilled water, methyl red ($C_{15}H_{15}N_3O_2$, 99% Merck), and tapioca starch. The equipment used in this research was an acrylic adsorption column with a diameter of 6 cm and a height of 30 cm, scanning electron microscopy/energy-dispersive X-ray spectroscopy (SEM/EDX, CARL ZEISS EVO MA 10), X-ray diffraction (XRD, Shimadzu XRD-6100), Fourier transform infrared (FTIR) spectroscopy (IR Prestige 21), oven (Memmert UN 30), UV-Vis Spectrophotometer (UV-1800), and a surface area analyzer.

2.2. Adsorbent and Adsorbate Preparation

The preparation of the bottom ash adsorbent began by weighing 100 g of bottom ash, which was then sieved using a 20-mesh sieve. An adhesive was prepared by mixing 15 g of tapioca starch with 45 mL of distilled water. The bottom ash was then mixed with the adhesive until a homogeneous mixture was formed and placed into an iron mold with a diameter of 1.5 cm and a height of 1 cm, representing a laboratory-scale process. The molded samples were oven-dried at 105°C until a constant weight was achieved. After drying, the adsorbent was removed from the mold and characterized using BET surface area analysis, SEM/EDX, XRD, and FTIR spectroscopy. The adsorbate solution was prepared by dissolving 20 mg of MR powder in a 1000 mL volumetric flask filled with distilled water to obtain a final concentration of 20 ppm.

2.3. Adsorption Process using Column

The adsorption process was conducted using an acrylic adsorption column with a diameter of 6 cm and a height of 30 cm. In the initial stage, the pre-formed and dried adsorbent was placed into the column, with bed heights varied at 4, 8, and 12 cm. Flow rates were adjusted to 5, 10, and 15 L/min, and adsorption times were set at 60, 120, and 180 minutes. A 20 ppm MR solution was introduced into the column in an up-flow manner, as illustrated in Figure 1. Samples were collected from the column via a valve at predetermined contact times and subsequently analyzed using a UV-Vis spectrophotometer. Table 1 presents the research variables.

The efficiency and adsorption capacity were calculated using Equations (1) and (2).

$$Removal\ efficiency\ (\%) = \frac{C_0 - C_e}{C_0} \times 100\% \tag{1}$$

$$q_t = \frac{V\,(C_0 - C_e)}{m} \tag{2}$$

Where, C_0 is the initial concentration of MR solution ($mg.L^{-1}$), C_e is the final concentration of MR solution ($mg.L^{-1}$), q_t is the adsorption capacity at time *t* ($mg.g^{-1}$), *m* is the adsorbent mass (g), *V* is volume of MR solution (L).

Table 1. Variables in research

Variable	Value
Bed heights, cm	4, 8, 12
Flow rates, L/min	5, 10, 15
MR concentration, ppm	20
Contact time variations, min	60, 120, 180

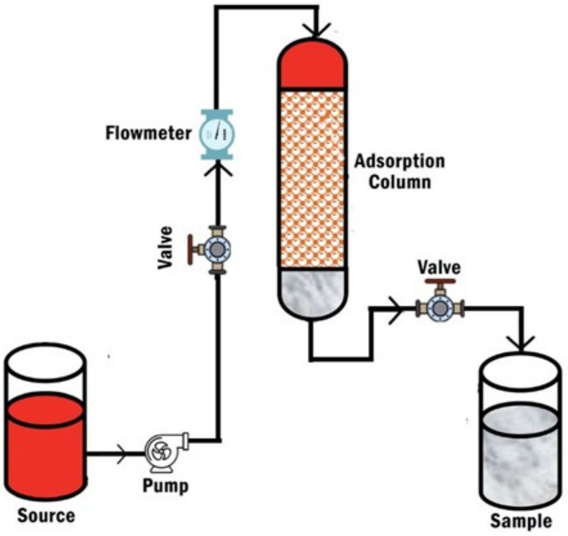

Figure 1. Schematic of the MR adsorption process using a bottom ash adsorbent in a column system

3. Results and Discussion

3.1. Adsorbent Characterization

The results of the bottom ash surface area analysis are shown in Table 2. The data indicate a relatively large surface area of 89.98 m^2/g, which enhances its adsorption capacity by providing more active sites for adsorption [20]. Figure 2 shows the structure and surface morphology of the adsorbent, analyzed by SEM at 500× magnification, with EDX used for elemental composition (Table 3). The results indicate that C, O, and Si are the dominant elements in the adsorbent, suggesting good adsorption potential due to their ability to interact with the dye's chemical structure and create favorable adsorption conditions. These elements contribute to adsorption through mechanisms such as electrostatic forces, hydrogen bonding, and hydrophobic interactions, all aiding MR uptake.

Figure 2a shows the SEM image of bottom ash before adsorption, revealing an average pore size of approximately 10 μm. In contrast, Figure 2b shows the adsorbent after adsorption, where the pores appear covered and more compact due to MR adsorption, indicating that the adsorbate has filled and blocked the pore spaces. BET analysis shows that the adsorbent derived from palm oil mill bottom ash has pores larger than 50 nm. Based on this pore size observed in the SEM analysis, the adsorbent is classified as a macroporous material. This classification aligns with other literature, which reports that bottom ash contains three types of pores: macropores (> 55 nm), mesopores (7–8 nm), and micropores (< 1 nm) [21, 22, 23].

The adsorbent was also identified using FTIR spectroscopy, with spectra recorded before and after adsorption, as shown in Figure 3. Identification is seen from the peaks that appear from several functional groups. Before adsorption, a peak at 958–954 cm^{-1} corresponds to the Si–O–Si bond, indicating the presence of silica in the bottom ash [21]. Another peak at 812 cm^{-1} represents the Al–O–Al bond, characteristic of alumina. Additionally, peaks at 1629–1504 cm^{-1} correspond to the bending vibrations of the –OH group, while the peak at 1696 cm^{-1} is attributed to C=O stretching.

Table 2. Physical properties of the bottom ash adsorbent

Sample	Pore volume (cm^3/g)	Specific surface area (m^2/g)	Pore size (nm)
Bottom ash	0.0032	89.801	58.523

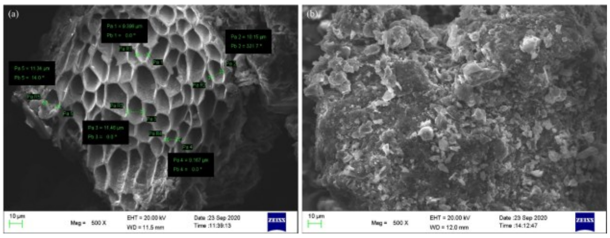

Figure 2. SEM images of the adsorbent (a) before and (b) after MR adsorption

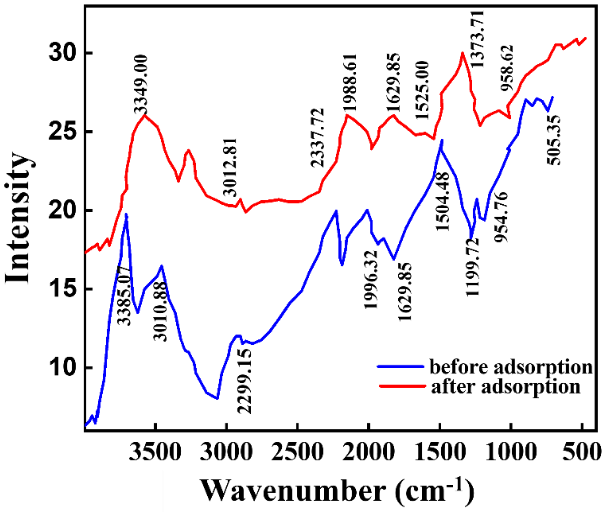

Figure 3. FTIR spectra of bottom ash before and after adsorption

Table 3. Physical properties of the bottom ash adsorbent

No	Element	Atom (%)	
		Before adsorption	After adsorption
1	C	45.77	33.63
2	O	36.9	45.13
3	Mg	1.01	0.95
4	Al	0.36	4.63
5	Si	11.88	8.63
6	P	0.55	0.3
7	K	1.88	4.04
8	Ca	1.36	2.05
9	Fe	0.28	0.64

After adsorption, spectral changes were observed. A peak at 3556 cm^{-1} corresponds to hydrogen bonding and hydroxyl groups, while stretches at 3468–3404 cm^{-1} indicate N–H stretching from aromatic primary amines. The peak at 3349 cm^{-1} is associated with azo bonds, while the peak at 1525 cm^{-1} corresponds to N=N stretching. Additionally, a peak at 1369 cm^{-1} represents the C–N bond of aromatic amines, and the peak at 1373.71 cm^{-1} is attributed to CH_3 and CH_2 bonding. These findings are consistent with previous FTIR analyses of MR adsorption on bottom ash, confirming successful adsorption [24].

3.2. Effects of Flow Rate, Contact Time, and Bed Height on MR Adsorption Efficiency and Capacity

Figure 4 illustrates the significant impact of MR flow rate and bed height on adsorption efficiency. A higher flow rate leads to lower adsorption efficiency, as the reduced contact time between MR and the adsorbent limits the adsorption process. Conversely, a lower flow rate allows for prolonged interaction, enhancing adsorption efficiency. As shown in Figure 6, the highest adsorption efficiency of 93% was achieved at a flow rate of 5 L/min and a bed height of 12 cm. This result is slightly different from the result obtained by Hamzah *et al.* [20], which is 98%.

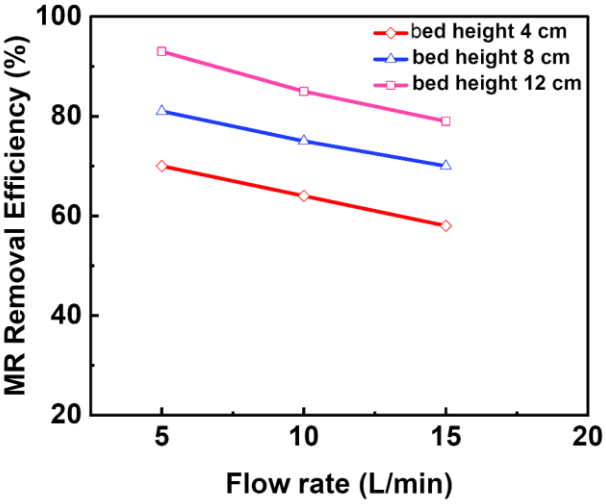

Figure 4. The effect of flow rate on the removal efficiency of MR

Figure 5 shows the relationship between contact time and separation efficiency, with adsorption durations from 60 to 180 minutes. The optimal contact time was observed at 180 minutes, achieving a maximum removal efficiency of 93% at a bed height of 12 cm. Contact time is a crucial factor in adsorption, as it determines the extent of interaction between the adsorbate and adsorbent. According to reaction rate theory, the reaction rate depends on the number of collisions occurring per unit of time [23]. Longer contact times increase collisions, driving the reaction toward equilibrium [24, 25]. The time required to reach adsorption equilibrium varies with the nature of adsorbent–adsorbate interactions.

The relationship between adsorption capacity and contact time is shown in Figure 6. Adsorption capacity increases with bed height due to the larger surface area and the availability of more active sites. At higher bed heights, a greater adsorbent surface area enhances MR adsorption capacity. The highest adsorption capacity of 0.850 mg/g was achieved at a contact time of 180 min and a bed height of 12 cm [11, 26, 27, 28, 29]. As contact time increases, more adsorbate accumulates on the adsorbent surface until equilibrium is reached. However, excessive contact time can lead to adsorbent saturation, preventing further adsorption and causing the release of adsorbate.

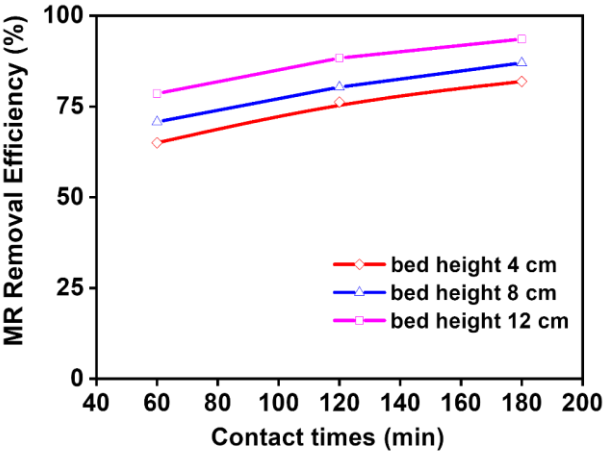

Figure 5. Effect of contact time and MR adsorption efficiency at different bed heights

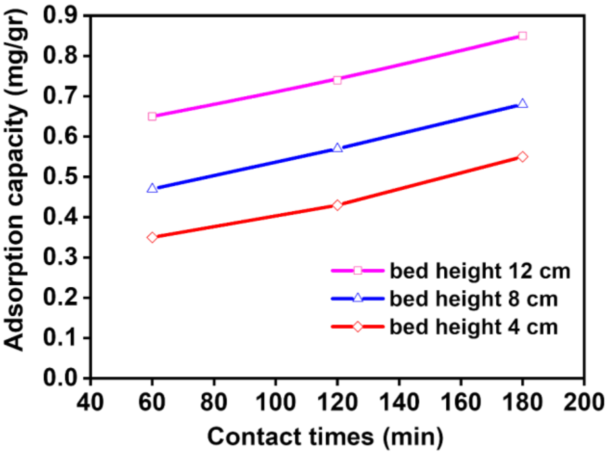

Figure 6. Effect of contact time and MR adsorption capacity at different bed heights

3.3. Adsorption Isotherm

Langmuir and Freundlich models were used to represent the adsorption equilibrium data in this study. The Langmuir model assumes that the adsorbent surface is homogeneous, with constant adsorption energy over the entire surface. This model also assumes that adsorption is localized, and each location can only absorb one molecule or atom, while the Freundlich adsorption isotherm model assumes that the adsorbate binding process occurs on heterogeneous surfaces [2, 13, 21, 28]. The isotherm models suitable for the equilibrium curves must be determined to optimize the sorption system design for MR sorption on bottom ash. In this study, the predicted values of the model and experimental data were validated by comparing the experimental adsorption capacity with the adsorption capacity estimated by this model through the coefficient of determination (R^2, a value close to or equal to 1 in Table 4). The MR adsorption isotherm model on bottom ash follows the Langmuir model shown in Figure 7 [8, 23, 26, 28].

Table 4. Langmuir and Freundlich isotherm parameters for MR adsorption onto bottom ash

Isotherm type	Parameter	Value	Equation form
Langmuir	q_m	0.889	$q = \frac{q_m K_L C_e}{1 + k_L C_e}$
	k_L	0.044	
	R^2	0.998	Non-linear
Freundlich	k_F	0.519	$q = k_f C_e^{\frac{1}{n}}$
	n	-1.812	
	R^2	0.815	Non-linear

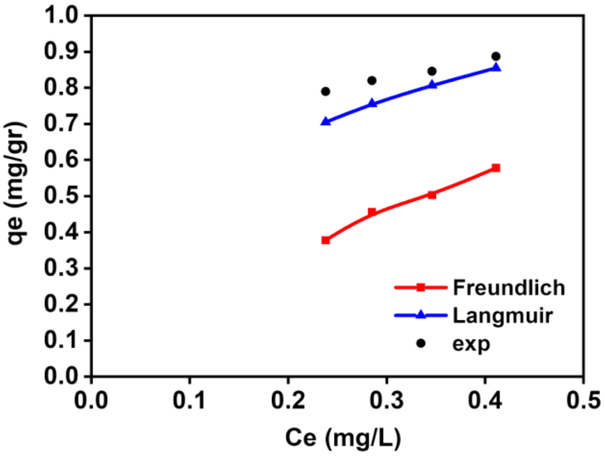

Figure 7. Adsorption isotherm of MR onto bottom ash

4. Conclusion

The research was conducted by varying the flow rate (5, 10, and 15 L/min), adsorbent bed height (4, 8, and 12 cm), and contact time (60, 120, and 180 minutes). The results showed that the highest adsorption efficiency, 93%, was achieved at a contact time of 180 minutes, a flow rate of 5 L/min, and a bed height of 12 cm. The highest adsorption capacity, 0.850 mg/g, was obtained at a bed height of 12 cm and a contact time of 180 minutes. The adsorption of MR using bottom ash follows the Langmuir isotherm model, as evidenced by the strong agreement between the model and experimental data, with an R^2 value of 0.998. These results indicate that bottom ash is a promising adsorbent for MR removal. Moreover, utilizing waste materials such as bottom ash offers a cost-effective source of raw materials and contributes to sustainable waste management solutions.

Acknowledgement

The authors are grateful to the Malikussaleh University of Chemical Engineering Simulation and Process Laboratory team.

References

[1] Kayode Adesina Adegoke, Olugbenga Solomon Bello, Dye sequestration using agricultural wastes as adsorbents, *Water Resources and Industry*, 12, (2015), 8-24 https://doi.org/10.1016/j.wri.2015.09.002

[2] Mohammad M. Hassan, Christopher M. Carr, A critical review on recent advancements of the removal of reactive dyes from dyehouse effluent by ion-exchange adsorbents, *Chemosphere*, 209, (2018), 201-219 https://doi.org/10.1016/j.chemosphere.2018.06.043

[3] Salma Gul, Mansha Kanwal, Raina Aman Qazi, Hajera Gul, Rozina Khattak, Muhammad Sufaid Khan, Fatima Khitab, Andrey E. Krauklis, Efficient Removal of Methyl Red Dye by Using Bark of Hopbush, *Water*, 14, 18, (2022), 2831 https://doi.org/10.3390/w14182831

[4] Muhammad Imran, David E. Crowley, Azeem Khalid, Sabir Hussain, Muhammad Waseem Mumtaz, Muhammad Arshad, Microbial biotechnology for decolorization of textile wastewaters, *Reviews in Environmental Science and Bio/Technology*, 14, 1, (2015), 73-92 https://doi.org/10.1007/s11157-014-9344-4

[5] Hinda Lachheb, Eric Puzenat, Ammar Houas, Mohamed Ksibi, Elimame Elaloui, Chantal Guillard, Jean-Marie Herrmann, Photocatalytic degradation of various types of dyes (Alizarin S, Crocein Orange G, Methyl Red, Congo Red, Methylene Blue) in water by UV-irradiated titania, *Applied Catalysis B: Environmental*, 39, 1, (2002), 75-90 https://doi.org/10.1016/S0926-3373(02)00078-4

[6] Simran Takkar, Bhawna Tyagi, Naveen Kumar, Taruna Kumari, Khushboo Iqbal, Ajit Varma, Indu Shekhar Thakur, Arti Mishra, Biodegradation of methyl red dye by a novel actinobacterium *Zhihengliuella* sp. ISTPL4: Kinetic studies, isotherm and biodegradation pathway, *Environmental Technology & Innovation*, 26, (2022), 102348 https://doi.org/10.1016/j.eti.2022.102348

[7] B. M. Vinoda, M. Vinuth, Y. D. Bodke, J. Manjanna, Photocatalytic degradation of toxic methyl red dye using silica nanoparticles synthesized from rice husk ash, *Journal of Environmental and Analytical Toxicology*, 5, 6, (2015), 1000336 http://dx.doi.org/10.4172/2161-0525.1000336

[8] Vanitha Katheresan, Jibrail Kansedo, Sie Yon Lau, Efficiency of various recent wastewater dye removal methods: A review, *Journal of Environmental Chemical Engineering*, 6, 4, (2018), 4676-4697 https://doi.org/10.1016/j.jece.2018.06.060

[9] Mohd Azmier Ahmad, Nur'Adilah Binti Ahmed, Kayode Adesina Adegoke, Olugbenga Solomon Bello, Sorption studies of methyl red dye removal using lemon grass (*Cymbopogon citratus*), *Chemical Data Collections*, 22, (2019), 100249 https://doi.org/10.1016/j.cdc.2019.100249

[10] José Arnaldo S. Costa, Caio M. Paranhos, Mitigation of silica-rich wastes: An alternative to the synthesis eco-friendly silica-based mesoporous materials, *Microporous and Mesoporous Materials*, 309, (2020), 110570 https://doi.org/10.1016/j.micromeso.2020.110570

[11] Yi Wai Chiang, Karel Ghyselbrecht, Rafael M. Santos, Boudewijn Meesschaert, Johan A. Martens, Synthesis of zeolitic-type adsorbent material from municipal solid waste incinerator bottom ash and its application in heavy metal adsorption, *Catalysis Today*, 190, 1, (2012), 23-30 https://doi.org/10.1016/j.cattod.2011.11.002

[12] Novi Sylvia, Rozanna Dewi, Ishak Ishak, Miftahul Janni, Melani Annisa Putri, Utilization of Fly Ash Palm Oil Mill Waste as an Adsorbent of Methylene Blue in a Fixed Bed Column System by Using Response Surface Methodology, *Jurnal Bahan Alam Terbarukan*, 13, 1, (2024), 28-37 https://doi.org/10.15294/jbat.v13i1.50001

[13] Wilson Wei Sheng Ho, Hoon Kiat Ng, Suyin Gan, Development and characterisation of novel heterogeneous palm oil mill boiler ash-based catalysts for biodiesel production, *Bioresource Technology*, 125, (2012), 158-164 https://doi.org/10.1016/j.biortech.2012.08.099

[14] Jasim Humadi, Amer T. Nawaf, Luay Ahmed Khamees, Yasser A. Abd-Alhussain, Hussain F. Muhsin, Mustafa A. Ahmed, Marwan M. Ahmed, Development of new effective activated carbon

supported alkaline adsorbent used for removal phenolic compounds, *Communications in Science and Technology*, 8, 2, (2023), 164-170 https://dx.doi.org/10.21924/cst

[15] Angga Pratama Herman, Suzana Yusup, Muhammad Shahbaz, David Onoja Patrick, Bottom Ash Characterization and its Catalytic Potential in Biomass Gasification, *Procedia Engineering*, 148, (2016), 432-436 https://doi.org/10.1016/j.proeng.2016.06.447

[16] Arti Malviya, Dipika Kaur Jaspal, Shraddha Khamparia, Kinetics studies on the adsorption of Methyl Orange and Metanil Yellow onto bottom ash: a comparative account, *Water Science and Technology*, 80, 10, (2019), 1844-1850 https://doi.org/10.2166/wst.2019.435

[17] Serpil Savcı, Mehmet Mert Uysal, Adsorption of Methylene Blue and Methyl Orange By Using Waste Ash, *Süleyman Demirel Üniversitesi Fen Bilimleri Enstitüsü Dergisi*, 21, 3, (2017), 831-835

[18] A. P. Wardanu, N. S. Indrasti, Suprihatin, Green Synthesis of Silica Nanoparticles (Si-NPs) from Palm Oil Fuel Ash (POFA) and its Application to Purification Water: A Review, *IOP Conference Series: Earth and Environmental Science*, 1358, 1, (2024), 012015 https://doi.org/10.1088/1755-1315/1358/1/012015

[19] Novi Sylvia, Fitriani Fitriani, Rozanna Dewi, Rizka Mulyawan, Abrar Muslim, Husni Husin, Yunardi Yunardi, Mutia Reza, Characterization of Bottom Ash Waste Adsorbent from Palm Oil Plant Boiler Burning Process to Adsorb Carbon Dioxide in a Fixed Bed Column, *Indonesian Journal of Chemistry*, 21, 6, (2021), 1454-1462 https://doi.org/10.22146/ijc.66509

[20] Muhammad Hazwan Hamzah, Muhammad Fitri Ahmad Asri, Hasfalina Che Man, Abdulsalam Mohammed, Prospective Application of Palm Oil Mill Boiler Ash as a Biosorbent: Effect of Microwave Irradiation and Palm Oil Mill Effluent Decolorization by Adsorption, *International Journal of Environmental Research and Public Health*, 16, 18, (2019), 3453 https://doi.org/10.3390/ijerph16183453

[21] Z. Ioannou, Ch. Karasavvidis, A. Dimirkou, V. Antoniadis, Adsorption of methylene blue and methyl red dyes from aqueous solutions onto modified zeolites, *Water Science and Technology*, 67, 5, (2013), 1129-1136 https://doi.org/10.2166/wst.2013.672

[22] Paul Egwuonwu DIM, Adsorption of methyl red and methyl orange using different tree bark powder, *SAVAP International*, 4, 1, (2013), 330-338

[23] Denga Ramutshatsha-Makhwedzha, Avhafunani Mavhungu, Mapula Lucey Moropeng, Richard Mbaya, Activated carbon derived from waste orange and lemon peels for the adsorption of methyl orange and methylene blue dyes from wastewater, *Heliyon*, 8, 8, (2022), e09930 https://doi.org/10.1016/j.heliyon.2022.e09930

[24] Khaled Mahmoudi, Khaled Hosni, Noureddine Hamdi, Ezzeddine Srasra, Kinetics and equilibrium studies on removal of methylene blue and methyl orange by adsorption onto activated carbon prepared from date pits-A comparative study, *Korean Journal of Chemical Engineering*, 32, 2, (2015), 274-283 https://doi.org/10.1007/s11814-014-0216-y

[25] Sunil Rajoriya, Virendra Kumar Saharan, Avdesh Singh Pundir, Mohit Nigam, Kuldeep Roy, Adsorption of methyl red dye from aqueous solution onto eggshell waste material: Kinetics, isotherms and thermodynamic studies, *Current Research in Green and Sustainable Chemistry*, 4, (2021), 100180 https://doi.org/10.1016/j.crgsc.2021.100180

[26] Tawfik A. Saleh, Akram A. Al-Absi, Kinetics, isotherms and thermodynamic evaluation of amine functionalized magnetic carbon for methyl red removal from aqueous solutions, *Journal of Molecular Liquids*, 248, (2017), 577-585 https://doi.org/10.1016/j.molliq.2017.10.064

[27] Robert Wolski, Aleksandra Bazan-Wozniak, Robert Pietrzak, Adsorption of Methyl Red and Methylene Blue on Carbon Bioadsorbents Obtained from Biogas Plant Waste Materials, *Molecules*, 28, 18, (2023), 6712 https://doi.org/10.3390/molecules28186712

[28] Kingsley O. Iwuozor, Joshua O. Ighalo, Ebuka Chizitere Emenike, Lawal Adewale Ogunfowora, Chinenye Adaobi Igwegbe, Adsorption of methyl orange: A review on adsorbent performance, *Current Research in Green and Sustainable Chemistry*, 4, (2021), 100179 https://doi.org/10.1016/j.crgsc.2021.100179

[29] Mohd Azmier Ahmad, Norhidayah Ahmad, Olugbenga Solomon Bello, Modified durian seed as adsorbent for the removal of methyl red dye from aqueous solutions, *Applied Water Science*, 5, 4, (2015), 407-423 https://doi.org/10.1007/s13201-014-0208-4

[30] Ying-Hong Guan, Jin Chen, Li-Jun Chen, Xin-Xin Jiang, Qiang Fu, Comparison of UV/H_2O_2, UV/PMS, and UV/PDS in Destruction of Different Reactivity Compounds and Formation of Bromate and Chlorate, *Frontiers in Chemistry*, 8, (2020), https://doi.org/10.3389/fchem.2020.581198

[31] Ruiyang Xiao, Lei He, Zonghao Luo, Richard Spinney, Zongsu Wei, Dionysios D. Dionysiou, Feiping Zhao, An experimental and theoretical study on the degradation of clonidine by hydroxyl and sulfate radicals, *Science of The Total Environment*, 710, (2020), 136333 https://doi.org/10.1016/j.scitotenv.2019.136333

[32] J. Rodríguez-Chueca, E. Laski, C. García-Cañibano, M. J. Martín de Vidales, Á Encinas, B. Kuch, J. Marugán, Micropollutants removal by full-scale UV-C/sulfate radical based Advanced Oxidation Processes, *Science of The Total Environment*, 630, (2018), 1216-1225 https://doi.org/10.1016/j.scitotenv.2018.02.279

[33] Pengfei Gan, Yichun Sun, Yunyi Li, Wen Liu, Jiangyu Ye, Meiping Tong, Jialiang Liang, The degradation of municipal solid waste incineration leachate by UV/persulfate and UV/H_2O_2 processes: The different selectivity of $SO_4^{\cdot-}$ and $\cdot OH$, *Chemosphere*, 311, (2023), 137009 https://doi.org/10.1016/j.chemosphere.2022.137009

[34] George Z. Kyzas, Nezamaddin Mengelizadeh, Morteza khodadadi Saloot, Samaneh Mohebi, Davoud Balarak, Sonochemical degradation of ciprofloxacin by hydrogen peroxide and persulfate activated by ultrasound and ferrous ions, *Colloids*

and Surfaces A: Physicochemical and Engineering Aspects, 642, (2022), 128627 https://doi.org/10.1016/j.colsurfa.2022.128627

[35] Jongbok Choi, Dukyoung Lee, Younggyu Son, Ultrasonic activation of persulfate for removal of aqueous pollutants: cavitational versus thermal mechanisms, *Current Opinion in Chemical Engineering*, 48, (2025), 101136 https://doi.org/10.1016/j.coche.2025.101136

[36] Xiuneng Zhu, Jie Qiu, Yexing Wang, Yulin Tang, Yongji Zhang, Effective Degradation of 1,4-Dioxane by UV-Activated Persulfate: Mechanisms, Parameters and Environmental Impacts, *Water*, 16, 9, (2024), 1281 https://doi.org/10.3390/w16091281

[37] David B. Miklos, Christian Remy, Martin Jekel, Karl G. Linden, Jörg E. Drewes, Uwe Hübner, Evaluation of advanced oxidation processes for water and wastewater treatment – A critical review, *Water Research*, 139, (2018), 118-131 https://doi.org/10.1016/j.watres.2018.03.042

[38] Marlo S. Morgan, Paul F. Van Trieste, Stephanie M. Garlick, Martin J. Mahon, Allan L. Smith, Ultraviolet molar absorptivities of aqueous hydrogen peroxide and hydroperoxyl ion, *Analytica Chimica Acta*, 215, (1988), 325-329 https://doi.org/10.1016/S0003-2670(00)85294-0

[39] Jaesang Lee, Urs von Gunten, Jae-Hong Kim, Persulfate-Based Advanced Oxidation: Critical Assessment of Opportunities and Roadblocks, *Environmental Science & Technology*, 54, 6, (2020), 3064-3081 https://doi.org/10.1021/acs.est.9b07082

[40] Kirill Fedorov, Kumaravel Dinesh, Xun Sun, Reza Darvishi Cheshmeh Soltani, Zhaohui Wang, Shirish Sonawane, Grzegorz Boczkaj, Synergistic effects of hybrid advanced oxidation processes (AOPs) based on hydrodynamic cavitation phenomenon – A review, *Chemical Engineering Journal*, 432, (2022), 134191 https://doi.org/10.1016/j.cej.2021.134191

[41] Ritesh Patidar, Vimal Chandra Srivastava, Mechanistic and kinetic insights of synergistic mineralization of ofloxacin using a sono-photo hybrid process, *Chemical Engineering Journal*, 403, (2021), 125736 https://doi.org/10.1016/j.cej.2020.125736

[42] Seungmin Na, Yun-Gyong Ahn, Mingcan Cui, Jeehyeong Khim, Significant diethyl phthalate (DEP) degradation by combined advanced oxidation process in aqueous solution, *Journal of Environmental Management*, 101, (2012), 104-110 https://doi.org/10.1016/j.jenvman.2012.01.028

[43] Oualid Hamdaoui, Emmanuel Naffrechoux, Sonochemical and photosonochemical degradation of 4-chlorophenol in aqueous media, *Ultrasonics Sonochemistry*, 15, 6, (2008), 981-987 https://doi.org/10.1016/j.ultsonch.2008.03.011

[44] Sanzeeda Baig Shuchi, Md Burhan Kabir Suhan, Sufian Bin Humayun, Muhammad Enamul Haque, Md Shahinoor Islam, Heat-activated potassium persulfate treatment of Sudan Black B dye: Degradation kinetic and thermodynamic studies, *Journal of Water Process Engineering*, 39, (2021), 101690 https://doi.org/10.1016/j.jwpe.2020.101690

[45] H. C. Yap, Y. L. Pang, S. Lim, A. Z. Abdullah, H. C. Ong, C. H. Wu, A comprehensive review on state-of-the-art photo-, sono-, and sonophotocatalytic treatments to degrade emerging contaminants, *International Journal of Environmental Science and Technology*, 16, 1, (2019), 601-628 https://doi.org/10.1007/s13762-018-1961-y

[46] Gholam Hossein Safari, Simin Nasseri, Amir Hossein Mahvi, Kamyar Yaghmaeian, Ramin Nabizadeh, Mahmood Alimohammadi, Optimization of sonochemical degradation of tetracycline in aqueous solution using sono-activated persulfate process, *Journal of Environmental Health Science and Engineering*, 13, (2015), 76 https://doi.org/10.1186/s40201-015-0234-7

[47] Linning Yin, Junyan Wei, Yumeng Qi, Zhengnan Tu, Ruijuan Qu, Chao Yan, Zunyao Wang, Feng Zhu, Degradation of pentachlorophenol in peroxymonosulfate/heat system: Kinetics, mechanism, and theoretical calculations, *Chemical Engineering Journal*, 434, (2022), 134736 https://doi.org/10.1016/j.cej.2022.134736

[48] Xiaofei Xue, Khalil Hanna, Mustapha Abdelmoula, Nansheng Deng, Adsorption and oxidation of PCP on the surface of magnetite: Kinetic experiments and spectroscopic investigations, *Applied Catalysis B: Environmental*, 89, 3, (2009), 432-440 https://doi.org/10.1016/j.apcatb.2008.12.024

[49] James R. Bolton, Keith G. Bircher, William Tumas, Chadwick A. Tolman, Figures-of-merit for the technical development and application of advanced oxidation technologies for both electric- and solar-driven systems (IUPAC Technical Report), *Pure and Applied Chemistry*, 73, 4, (2001), 627-637 https://doi.org/10.1351/pac200173040627

[50] Mohammad A. Behnajady, Behrouz Vahid, Nasser Modirshahla, Mohammad Shokri, Evaluation of electrical energy per order (E_{EO}) with kinetic modeling on the removal of Malachite Green by US/UV/H_2O_2 process, *Desalination*, 249, 1, (2009), 99-103 https://doi.org/10.1016/j.desal.2008.07.025

[51] Kaiheng Guo, Zihao Wu, Shuwen Yan, Bo Yao, Weihua Song, Zhechao Hua, Xuewen Zhang, Xiujuan Kong, Xuchun Li, Jingyun Fang, Comparison of the UV/chlorine and UV/H_2O_2 processes in the degradation of PPCPs in simulated drinking water and wastewater: Kinetics, radical mechanism and energy requirements, *Water Research*, 147, (2018), 184-194 https://doi.org/10.1016/j.watres.2018.08.048

[52] Menghong Gao, Shuili Yu, Li'an Hou, Xingli Ji, Rongsheng Ning, Ying Xu, Lei Li, Treatment of emerging pyrrolizidine alkaloids in drinking water by UV/persulfate process: Kinetics, energy efficiency and degradation pathway, *Chemical Engineering Journal*, 490, (2024), 151852 https://doi.org/10.1016/j.cej.2024.151852